CRYSTAL GROWTH & DESIGN

Article

pubs.acs.org/crystal

High Solubility Piperazine Salts of the Nonsteroidal Anti-Inflammatory Drug (NSAID) Meclofenamic Acid

Palash Sanphui, Geetha Bolla, and Ashwini Nangia*

School of Chemistry, University of Hyderabad, Prof. C. R. Rao Road, Gachibowli, Central University P.O., Hyderabad 500046, India

Supporting Information

ABSTRACT: Meclofenamic acid (MFA) is the most potent anti-inflammatory drug among the fenamic acids. We report (1) two cocrystals of MFA with isonicotinamide (INA) and 4,4′-bipyridine (BPY); (2) polymorphs of MFA and piperazine (PPZ) 1:1 salt (orthorhombic $P2_12_12_1$ O and monoclinic $P2_1/c$ M), MFA−PPZ−H_2O 1:1:1 salt hydrate, MFA−PPZ 2:1 salt; and (3) MFA and 2-aminopyridine (2-APY) 1:1 salt, MFA and 4-aminopyridine (4-APY) 1:1:1 salt hydrate. Sublimation of MFA gave single crystals for X-ray diffraction which provided good quality data for refinement and all atomic coordinates. The cocrystal and salt structures are assembled via neutral O−H···O, O−H···N, N−H···O, N−H···N, and ionic O−H···O^-, N^+−H···O^- hydrogen bonds. The disorder of the methyl group in the MFA crystal structure is absent in the cocrystal and salt structures, which contain different conformers (A or B) of methyl group orientation. The solubility of MFA−INA (1:1) and MFA−BPY (1:0.5) cocrystals is 2.9 and 7.6 times higher than that of MFA at 37 °C in 50% EtOH−water. Interestingly, MFA−PPZ-M 1:1 salt and its 1:1:1 hydrate are 2724- and 1334-fold more soluble than MFA. Both of these salts transformed in 50% EtOH−water slurry at 37 °C to MFA−PPZ 2:1 salt after 24 h, which in turn transformed to MFA after another 24 h of slurry stirring. Remarkably, the dissolution rate of MFA−PPZ-M (1:1) salt in water is just slightly lower than that of the marketed sodium meclofenamate.

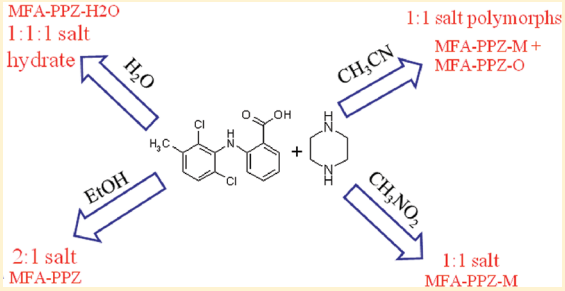

INTRODUCTION

About 40% of new molecular entities coming out of the drug discovery pipeline will never advance in the development chain because of biopharmaceutical issues, such as poor aqueous solubility, low dissolution rate, low permeability, and first-pass metabolism in the liver. An enhancement of drug solubility for therapeutic agents can improve their bioavailability. Identifying the optimum solid form of an active pharmaceutical ingredient (API) is always desirable for clinical use.[1] Over 80% of all drugs are marketed as tablets, and oral administration is the most preferred drug delivery route. Different solid-state forms, such as polymorphs, amorphous, cocrystals, salts, and their hydrates, can be crystallized to improve physicochemical properties of drug substances. Crystal engineering is particularly well suited to cocrystallization of drugs with safe coformers.[2] The advantage of cocrystals and salts for improving physical properties such as solubility, bioavailability, stability, etc.[3] is that the structure of the drug molecule is unchanged but the modification is at the supramolecular level (intermolecular interactions, hydrogen bonding, molecular packing). A practical advantage is that the extent of solubility enhancement for cocrystals (4−20 times) is an order of magnitude higher than that for polymorphs (2−3 times). Pharmaceutical salts of course are the most preferred formulation for solubility enhancement (100−1000 times).[4] On the downside, salts are more likely to form hydrates (often a drawback in terms of stability) compared to cocrystals. The ΔpK_a rule, wherein $\Delta pK_a = pK_a$ (conjugate acid of base) − pK_a (acid), is a useful guide to know beforehand if an acid−base complex will give a neutral cocrystal ($\Delta pK_a < 3$) or an ionic salt ($\Delta pK_a > 3$). A more practical cutoff for organic salts is $\Delta pK_a < 0$ for cocrystal, $\Delta pK_a > 3$ for salts, and the range $0 < \Delta pK_a < 3$ being an unpredictable zone wherein multiple proton states could be observed.[5]

Meclofenamic acid (MFA)[6] (Figure 1) is a nonsteroidal anti-inflammatory, antipyretic, analgesic drug used in the treatment of postoperative and traumatic inflammation and swelling by the inhibition of prostaglandin biosynthesis pathway.[6a] It is a selective cyclo-oxygenase-2 (COX-2) inhibitor.[6b] Similar to

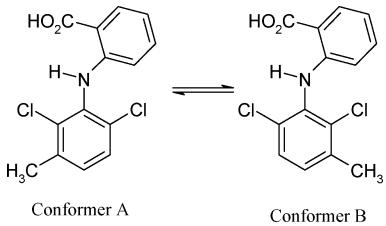

Figure 1. Two conformers (A and B) of meclofenamic acid (MFA) present in crystal structures.

Received: January 2, 2012
Revised: February 17, 2012
Published: February 24, 2012

diclofenac, MFA is also used as a KCNQ2/Q3 potassium channel opener, depressor of cortical neuron activity, and exhibits anticonvulsant activity.[6e] MFA also has a transient effect on platelet aggregation, but unlike aspirin, it does not cause bleeding.[6h] It is a BCS class II drug of low solubility (30 mg/L) and high permeability (log P_{ow} = 5).[7] Novel gel and cream formulations of MFA provide maximal topical activity to the drug.[6e] Exposure of dilute solutions of MFA to visible or UV light resulted in fairly rapid decomposition.[6f] Because of its low aqueous solubility[7] and thus bioavailability, the sodium salt of MFA (solubility > 250 g/L)[7b] is sold commercially as 100 mg capsules under brand names Meclomen, Melvon, Movens, and Arquel. Fábián et al.[8] recently published cocrystals of flufenamic acid, niflumic acid, tolfenamic acid, and mefenamic acid with nicotinamide, but they mentioned some difficulty with MFA. Our results on cocrystals and salts of MFA demonstrate that organic salts of APIs can exhibit comparable dissolution rates to traditional metal ion salts. The novel cocrystals and salts of MFA with isonicotinamide (INA), 4,4′-bipyridine, piperazine, aminopyridine, etc. were prepared by solvent-assisted grinding, and their solubility was measured in a USP dissolution tester. Crystal structures, phase transformations, and solubility of MFA cocrystals and salts are discussed.

RESULTS AND DISCUSSION

The sodium salt of MFA was obtained from Sigma-Aldrich, India, and converted to the free acid with aq. HCl. The Na salt of MFA is readily soluble in water. Vijayan et al.[9] (1981) published the first crystal structure of MFA but it had a high *R*-factor of 0.135. The same authors reported crystal structure of the 1:1 complex of MFA with choline hydrate and ethanolamine.[10] The disorder in the methyl group orientation of MFA (Figure 1) persisted at low temperature. We have now obtained good quality single crystals of MFA by sublimation and collected data at 298 and 100 K. There are no reports on crystal structures of MFA and its salt/cocrystal in the interim period. Crystallographic parameters for all crystal structures are listed in Table 1. ORTEP diagrams are displayed in Figure S1, Supporting Information.

CRYSTAL STRUCTURE DESCRIPTION

Meclofenamic Acid (MFA). MFA consists of two aryl moieties, the *N*-2,6-dichloro-3-methylphenyl group and the *N*-2-benzoic acid group. The aryl rings are twisted almost in a perpendicular orientation of an 82° dihedral angle between the two ring planes. This twist relieves steric congestion of ortho-substituted phenyls at the secondary amine. MFA was crystallized by slow sublimation at 190−200 °C over 4−5 h to afford diffraction quality single crystals which was solved in the triclinic space group $P\bar{1}$ with one molecule in the asymmetric unit. Similar to other fenamic acids, for example, mefenamic acid and tolfenamic acid,[11] two MFA molecules form a centrosymmetric carboxylic acid dimer of O−H···O hydrogen bond (O···O, 2.632(4) Å) in the $R_2^2(8)$ ring motif.[12] An intramolecular N−H···O hydrogen bond (N···O, 2.679(4) Å) of $R_1^1(6)$ ring motif (Figure 2) rigidifies the molecule. Hydrogen bond parameters in crystal structures are listed in Table 2. The 3-methyl group is disordered over two positions with unequal site occupancy factor (sof conformer *B* = 0.58(1) and *A* = 0.42(1); see Figure 1) at 298 K (RT structure). X-ray reflections for MFA crystal were collected at 100 K (LT structure) in an attempt to resolve the disorder issue (*R*-factor 0.110). The disorder of the Me group persisted, now with sof of conformer *B* = 0.577(15) and *A* = 0.423(15). The elongated thermal ellipsoid of Cl2 (chlorine atom 2) perpendicular to the aromatic plane in the RT structure could be modeled as Cl2A and Cl2B (chlorine 2A and 2B) with sof of 0.55(3) and 0.45(3) in the LT structure. The RT structure of MFA is described in this paper because it has better refinement parameters and lower *R*-factor (0.083).

Meclofenamic Acid−Isonicotinamide Cocrystal (1:1, MFA−INA). MFA−INA (1:1) cocrystal was prepared by solid-state grinding, and the resulting solid was crystallized from acetonitrile to afford the single crystal X-ray structure in monoclinic space group $P2_1/c$, which contained conformer A of MFA. The carboxylic acid dimer in the reference drug crystal structure is replaced by carboxylic acid−pyridine heterosynthon (O···N, 2.657(4) Å, ∠O−H···N, 174°) as the main bimolecular $R_2^2(7)$ ring motif (Figure 3a). Different synthons present in the novel solid phases are displayed in Scheme 1. INA molecules aggregate via the carboxamide dimer (N···O, 2.926(4) Å, ∠N−H···O, 169°) at the secondary level. Such 4-molecule supramolecular units are connected via C−Cl···O interaction (3.25 Å) in a ladder motif along the *b*-axis (Figure 3b).

Meclofenamic Acid−4,4′-Bipyiridine Cocrystal (1:0.5, MFA−BPY). MFA−BPY (1:0.5) cocrystal (crystallized from acetonitrile) was solved in monoclinic space group $P2_1/c$ and contains MFA conformer A. The acid−pyridine heterosynthon (O···N, 2.668(4) Å, ∠O−H···N, 178°; $R_2^2(7)$ ring motif) is supported by an auxiliary C−H···O hydrogen bond (C···O, 3.194(6) Å) between the pyridine ortho C−H to the carbonyl of carboxylic acid (Figure 4a). The trimolecular units in the cocrystal make a stepladder motif along the *c*-axis (Figure 4b). MFA−BPY (1:1) is a cocrystal based on C−O bond distances of 1.215(8) Å and 1.316(7) Å in the carboxylic acid group and ∠C−N−C bond angle of 115.7(5)° in the pyridine ring.

Piperazinium Meclofenamate Salt Polymorphs (1:1, MFA−PPZ-M and MFA−PPZ-O). Piperazinium meclofenamate salt (1:1) crystallized as monoclinic ($P2_1/c$) and orthorhombic ($P2_12_12_1$) polymorphs concomitantly from acetonitrile solvent. There is one molecule each of meclofenamate anion (conformer B) and piperazinium cation in the asymmetric unit. Compared to the cocrystal, proton transfer occurred in the salt structure from carboxylic acid to the N−H base of piperazine. In the monoclinic structure (MFA−PPZ-M), each piperazine molecule forms four hydrogen bonds with two meclofenamates and two piperazinium cations through ionic $N^+-H\cdots O^-$ (N···O, 2.677(4) Å) and neutral N−H···N (N···N, 2.851(4) Å) and N−H···O (N···O, 2.949(4) Å) hydrogen bonds (Figure 5a). The carboxylate C−O bond distances are 1.236(4) Å and 1.271(4) Å and piperazinium ∠C−N−C is 112.0(3)° suggesting an ionized species. The C−O bond distances difference (ΔCO) is less than 0.1 Å compared to the neutral species.

The packing of meclofenamate anions (conformer A) and piperazinium cations is similar in the orthorhombic polymorph (MFA−PPZ-O). Each piperazine molecule forms four hydrogen bonds with two meclofenamate anions and two piperazinium cations through $N^+-H\cdots O^-$ (2.698(3) Å), N−H···N (2.858 (3) Å), and N−H···O (2.960 (3) Å) hydrogen bonds (Figure 5b). C−O bond distances (1.226(6) Å, 1.263(5) Å) and ∠C−N−C angle (111.8(3)°) are consistent with a salt species.[5] In both polymorphs, six piperazine cations are sandwiched between three meclofenamate anions along the *c*-axis. A minor difference between the two polymorphs is the orientation of the methyl group in MFA, that is, conformer

dx.doi.org/10.1021/cg300002p | Cryst. Growth Des. 2012, 12, 2023−2036

Table 1. Crystallographic Parameters of MFA and Its Cocrystals and Salts

	MFA-100K	MFA-RT	MFA−INA (1:1)	MFA−BPY (1:0.5)	MFA−PPZ-M (1:1)
empirical formula	$C_{14}H_{10}Cl_2NO_2$	$C_{14}H_{10}Cl_2NO_2$	$C_{14}H_{11}Cl_2NO_2{\cdot}C_6H_6N_2O$	$C_{14}H_{11}Cl_2{\cdot}0.5(C_{10}H_8N_2)$	$C_{14}H_{10}Cl_2NO_2{\cdot}C_4H_{11}N_2$
formula weight	295.13	295.13	418.27	374.23	382.28
crystal system	triclinic	triclinic	monoclinic	monoclinic	monoclinic
space group	$P\bar{1}$	$P\bar{1}$	$P2_1/c$	$P2_1/c$	$P2_1/c$
T (K)	100	298	298	298	298
a (Å)	8.5209(11)	8.566(3)	7.5327(13)	7.4180(6)	16.3805(13)
b (Å)	8.8775(11)	8.968(3)	31.313(5)	8.2144(6)	8.3717(5)
c (Å)	9.1986(12)	9.378(3)	9.601(3)	28.770(2)	14.4609(11)
α (°)	104.265(2)	103.090(6)	90	90	90
β (°)	103.337(2)	103.194(6)	121.439(16)	97.099(7)	102.347(8)
γ (°)	91.569(2)	92.538(6)	90	90	90
V (Å^3)	653.56(14)	679.7(4)	1932.2(7)	1739.6(2)	1934.8(3)
D_{calcd} (g cm^{-3})	1.500	1.442	1.438	1.429	1.312
μ (mm^{-1})	0.492	0.473	0.363	0.388	0.351
θ range	2.36−25.89	2.47−25.77	2.59−29.03	2.75−29.10	2.74−26.31
Z	2	2	4	4	4
range h	−9 to +9	−9 to +9	−9 to +9	−8 to +8	−20 to +20
range k	−10 to +10	−10 to +10	−39 to +39	−9 to +9	−10 to +10
range l	−10 to +10	−10 to +10	−11 to +12	−31 to +31	−18 to +18
reflections collected	5863	6239	9616	8621	8452
total reflections	2153	2227	3944	2487	3956
observed reflections	1954	1698	1932	1726	1574
R_1 [$I > 2\sigma(I)$]	0.1106	0.0833	0.0567	0.0892	0.0641
wR_2 (all)	0.2193	0.1910	0.1547	0.2088	0.1850
goodness-of-fit	1.209	1.122	0.915	1.127	0.933
diffractometer	SMART BRUKER	SMART BRUKER	Oxford CCD	Oxford CCD	Oxford CCD
	MFA−PPZ- O (1:1)	MFA−PPZ (2:1)	MFA−PPZ−H_2O (1:1:1)	MFA−2-APY (1:1)	MFA−4-APY−H_2O (1:1:1)
empirical formula	$C_{14}H_{10}Cl_2NO_2{\cdot}C_4H_{11}N_2$	$2(C_{14}H_{10}Cl_2\ NO_2){\cdot}C_4H_{12}N_2$	$C_{14}H_{10}Cl_2NO_2{\cdot}C_4H_{11}N_2{\cdot}H_2O$	$C_{14}H_{10}Cl_2NO_2\ {\cdot}C_5H_7N_2$	$C_{14}H_{10}Cl_2NO_2{\cdot}C_5H_7N_2{\cdot}H_2O$
formula weight	382.28	678.42	400.29	390.26	408.27
crystal system	orthothombic	triclinic	monoclinic	monoclinic	monoclinic
space group	$P2_12_12_1$	$P\bar{1}$	$P2_1/c$	$P2_1/n$	$P2_1/c$
T (K)	298	298	298	298	298
a (Å)	7.929(3)	7.9109(3)	16.137(4)	14.675(4)	16.227(4)
b (Å)	8.168(3)	11.1289(4)	8.4889(15)	7.1318(15)	8.4770(15)
c (Å)	28.381(15)	18.1180(7)	15.596(3)	18.605(6)	15.686(4)
α (°)	90	81.943(3)	90	90	90
β (°)	90	80.424(4)	114.94(3)	110.73(3)	116.18(3)
γ (°)	90	88.809(3)	90	90	90
V (Å^3)	1838.1(13)	1557.36(11)	1937.1(7)	1821.2(8)	1936.2(7)
D_{calcd} (g cm^{-3})	1.381	1.447	1.373	1.423	1.401
μ (mm^{-1})	0.370	0.425	0.358	0.375	0.360
θ range	2.86−26.31	2.74−26.31	2.77−24.71	2.77−29.22	2.78−26.37
Z	4	2	4	4	4
range h	−9 to +9	−9 to +9	−18 to +18	−18 to +18	−20 to +20
range k	−10 to +10	−13 to +13	−9 to +9	−8 to +8	−10 to +10
range l	−35 to +35	−22 to +22	−18 to +18	−23 to +23	−19 to +19
reflections collected	5203	12514	6934	7324	8218
total reflections	3366	6346	3283	3721	3958
observed reflections	1540	3882	1942	2081	2641
R_1 [$I > 2\sigma(I)$]	0.0597	0.0687	0.0868	0.0459	0.0609
wR_2 (all)	0.0663	0.1770	0.2540	0. 1228	0.1608
goodness-of-fit	0.865	1.030	1.046	0.919	1.038
diffractometer	Oxford CCD	Oxford CCD	Oxford CCD	Oxford CCD	Oxford CCD

A or B. Piperazine is a small cyclic diamine that is pharmaceutically acceptable and has anthelmintic activity.[13] Piperazine (pK_a = 9.72) can act both as a neutral and a cationic coformer to give a cocrystal or salt product with an acidic API. The Cambridge Structural Database (CSD ver. 5.32, 2010, November 2011 update)[14] contains about 20 organic cocrystals and 25 salts or salt hydrates of piperazine (Table S1, Supporting Information). Surprisingly, there is only one piperazinium

dx.doi.org/10.1021/cg300002p | Cryst. Growth Des. 2012, 12, 2023−2036

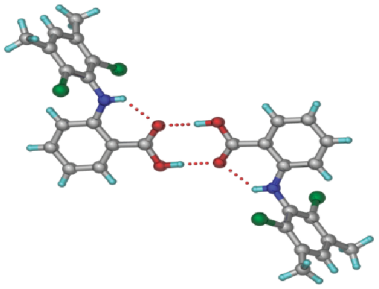

Figure 2. Centrosymmetric carboxylic acid dimer in MFA. The methyl group is disordered in the crystal structure of MFA with sof 0.58(1) and 0.42(1).

monocation (Refcode CUKVOU) listed with a carboxylate counterion up to the recent update of the CSD; there are 73 refcodes for piperazinium dication (Table S2, Supporting Information). We report three piperazinium monocations with meclofenamate anion in MFA−PPZ-M, MFA−PPZ-O, and MFA−PPZ−H_2O crystal structures. Furthermore, there are no examples of piperazine salts which are polymorphic. MFA−PPZ (1:1) is the first example of piperazine salt polymorphs with 3D coordinates determined. Crystal density (1.312, 1.381 g cm^{-3}), packing fraction (64.2, 68.0%, calculated in Platon), and lattice energy (−176.93, −186.39 kcal mol^{-1}, calculated using Compass force field in Cerius^2)[15] of monoclinic and orthorhombic polymorphs suggest that the orthorhombic form should be

Table 2. Hydrogen Bonds in Crystal Structures (Neutron-Normalized Distances)

crystal forms	interaction	H···A (Å)	D···A (Å)	∠D−H···A (°)	symmetry code
MFA	N1−H1··· O1	1.95	2.679 (4)	126	intramolecular
	O2−H2··· O1	1.66	2.632 (4)	171	$1-x, 2-y, -z$
MFA−INA	N1−H1··· O1	1.83	2.653(4)	137	intramolecular
	O2−H2··· N3	1.68	2.657(4)	174	$x, y, -1+z$
	N2−H2A··· O3	1.93	2.926(4)	169	$1-x, -y, 1-z$
MFA−BPY	N1−H1··· O1	1.84	2.640(4)	133	intramolecular
	O2−H2··· N2	1.69	2.668(4)	178	$x, -1+y, z$
	C15−H15···O1	2.41	3.194(4)	129	$x, 1+y, z$
MFA−PPZ-M	N1−H1··· O1	1.75	2.604(4)	140	intramolecular
	N2−H2··· O1	1.68	2.677(4)	171	$x, 1/2-y, 1/2+z$
	N2−H2··· O2	2.53	3.231(4)	126	$x, 1/2-y, 1/2+z$
	N2−H2A··· N3	1.89	2.851(4)	159	$-x, -1/2+y, 1/2-z$
	N3−H3A··· O2	1.99	2.949(4)	157	$x, 3/2-y, 1/2+z$
MFA−PPZ-O	N1−H1··· O1	1.79	2.619(3)	137	intramolecular
	N2−H2··· O1	1.71	2.698(3)	164	$1-x, 1/2+y, 1/2-z$
	N2−H2··· O2	2.48	3.246(3)	133	$1-x, 1/2+y, 1/2-z$
	N2−H2A··· N3	1.85	2.858(3)	178	$1/2+x, 1/2-y, -z$
	N3−H3A··· O2	1.97	2.960(3)	165	$-x, 1/2+y, 1/2-z$
	C6−H6··· Cl1	2.71	3.201(4)	107	intramolecular
MFA−PPZ (2:1)	N1−H1··· O1	2.05	2.682 (3)	119	intramolecular
	N2−H2··· O3	1.99	2.642 (3)	120	intramolecular
	N3−H3A··· O1	1.70	2.690(3)	164	$1-x, 1-y, 1-z$
	N3−H3B··· O4	1.74	2.731(3)	167	$1-x, -y, 1-z$
	N4−H4A··· O2	1.77	2.750(3)	162	$-1+x, y, z$
	N4−H4B··· O3	1.72	2.695(3)	162	$1-x, 1-y, 1-z$
	C29−H29B···O3	2.49	3.318(3)	132	$1-x, 1-y, 1-z$
	C32−H32B···Cl3	2.67	3.446(3)	128	$1-x, 1-y, 1-z$
MFA−PPZ−H_2O	N1−H1···O1	1.91	2.699(3)	133	intramolecular
	N3−H1A···N2	1.99	2.939(4)	155	$1-x, 1/2+y, 1/2-z$
	N3−H1B···O1	1.90	2.842(4)	154	$x, 1/2-y, -1/2+z$
	N2−H2···O3	2.10	3.029(4)	152	$1-x, -1/2+y, 1/2-z$
	O3−H3A···O1	1.87	2.796(4)	155	x, y, z
	O3−H3B···O2	1.72	2.692(4)	170	$1-x, -y, 1-z$
	C16−H16B···O2	2.43	3.488(4)	167	$1-x, -y, 1-z$
	C17−H17B···O3	2.35	3.356(4)	155	$1-x, 1/2+y, 1/2-z$
	C3−H3···Cl1	2.67	3.607(4)	145	$x, -1/2-y, 1/2+z$
MFA−2-APY	N1−H1···O1	1.88	2.631(3)	128	intramolecular
	N2−H2···O1	1.64	2.642(3)	175	$1-x, -y, -z$
	N3−H3A···O2	1.84	2.841(3)	173	$1-x, -y, -z$
	N3−H3B···O2	1.92	2.897(3)	164	$-1/2+x, 1/2-y, 1/2+z$
MFA−4-APY−H_2O	N1−H1···O2	1.79	2.603(4)	135	intramolecular
	N2−H2···O3	1.92	2.837(4)	149	$x, 1/2-y, 1/2+z$
	N3−H3A···O1	2.07	3.017(4)	156	$1-x, 1/2+y, 1/2-z$
	N3−H3B···O3	2.00	2.993(4)	169	$x, 3/2-y, 1/2+z$
	O3−H3C···O1	1.78	2.761(4)	173	$x, 1/2-y, -1/2+z$
	O3−H3D···O2	1.75	2.713(4)	166	$1-x, -1/2+y, 1/2-z$
	C17−H17···O1	2.48	3.301(4)	131	$1-x, 1-y, 1-z$

dx.doi.org/10.1021/cg300002p | *Cryst. Growth Des.* 2012, 12, 2023−2036

more stable. However, differential scanning calorimetry (DSC) measurements (discussed later) indicate that the melting point of the monoclinic form is higher and we show that MFA−PPZ-M is the stable polymorph.

Piperazinium Meclofenamate Salt (2:1, MFA−PPZ). Piperazinium meclofenamate salt (2:1) was obtained when the components were ground with a few drops of EtOH added. The crystal structure of MFA−PPZ (2:1) was solved in $P\bar{1}$ space group with two crystallographic meclofenamate anions (conformer A and B) and two half piperazinium cations in the asymmetric unit. The two conformers of MFA are arranged in an alternate fashion ABAB parallel to the *b*-axis, and piperazinium cations are sandwiched between the anion layers. Each piperazinium dication forms four N^+−H···O^- ionic hydrogen bonds ($N3^+$−H3A···$O1^-$, 2.690(3) Å; $N3^+$−H3B···$O4^-$, 2.731(3) Å; $N4^+$−H4A···$O2^-$, 2.750(3) Å and $N4^+$−H4B···$O3^-$, 2.695(3) Å with meclofenamate anions A and B (shown in thick bond and ball and stick models, Figure 6). This is the only crystal structure of MFA salts with both conformers A and B in the same lattice.

Piperazinium Meclofenamate Salt Hydrate (1:1:1, MFA−PPZ−H_2O). Piperazinium meclofenamate salt hydrate (1:1:1) was obtained during grinding of MFA with piperazine hydrate or MFA and piperazine in the presence of water. It crystallized in the monoclinic space group $P2_1/c$ with conformer B.

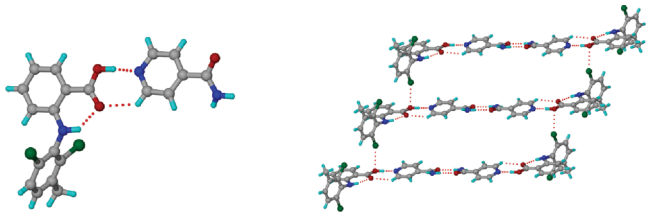

Figure 3. (a) Acid−pyridine heterosynthon in MFA−INA (1:1) cocrystal. (b) Acid−pyridine heterosynthon, amide dimer homosynthon, and C−Cl···O interaction along the *b*-axis in crystal structure.

Two meclofenamate anions and two water molecules form ring motif of graph set notation $R_4^4(12)$. Water molecules are present as spacers between two meclofenamates. Two piperazinium cations form N^+−H···O hydrogen bonds ($N2^+$−H2···O3, 3.029(4) Å) with water (Figure 7a). The N−H···N/O hydrogen bond network ($N3^+$−H1B···$O1^-$, 2.842(4) Å, $N3^+$−H1A···N2, 2.939(4) Å) is shown in Figure 7b. Water molecules reside in channels along the *c*-axis (Figure 7c). Thermogravimetric analysis (TGA) (Figure S2, Supporting Information) confirmed

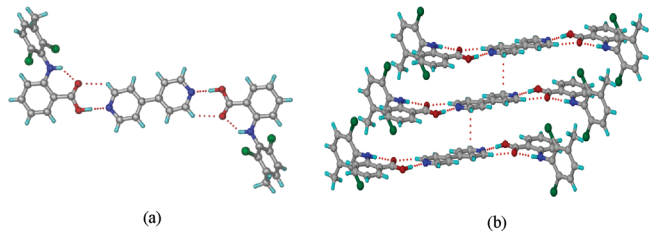

Figure 4. (a) Acid−pyridine heterosynthon form termolecular unit in MFA−BPY (1:0.5) cocrystal structure. (b) Ladder structure along the *c*-axis.

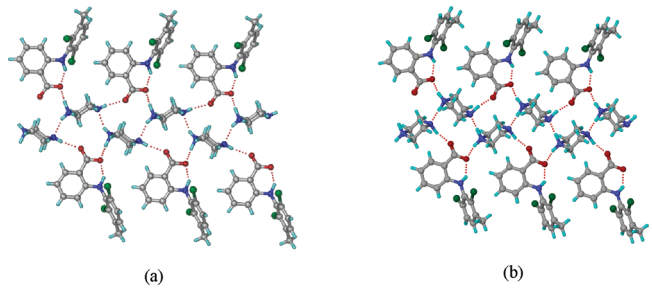

Figure 5. Crystal packing in (a) monoclinic form of MFA−PPZ-M (1:1) viewed along the *b*-axis, and (b) orthorhombic polymorph MFA−PPZ-O (1:1) along the *a*-axis. The main difference is in the orientation of Me group in MFA, that is, conformer B (in M) and A (in O).

Scheme 1. Different Hydrogen Bond Synthons in Crystal Structures[a]

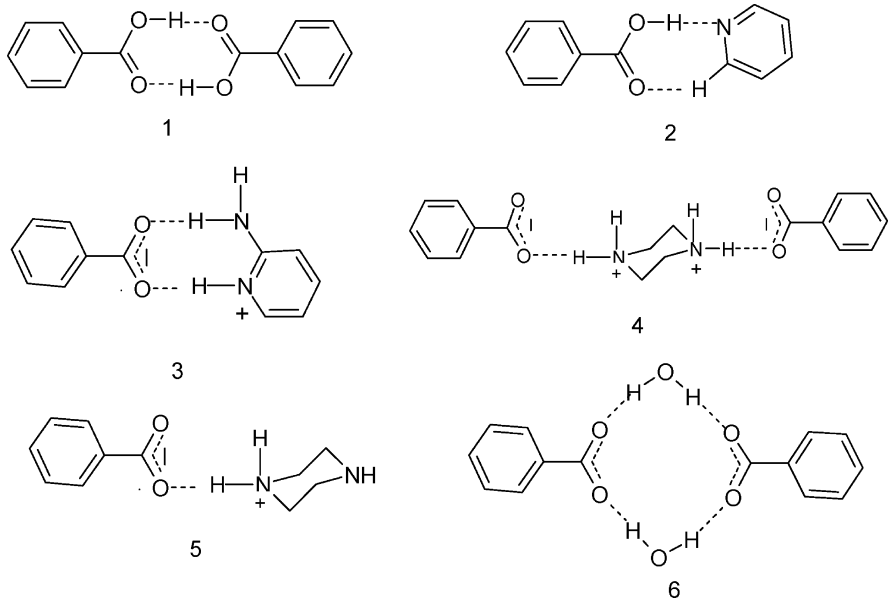

[a](1) Acid−acid dimer $R_2^2(8)$, (2) acid−pyridine $R_2^2(7)$ ring motif, (3) carboxylate−aminopyridinium $R_2^2(8)$ ring motif, (4) carboxylate−piperazinium−carboxylate salt, (5) carboxylate−piperazinium salt, (6) carboxylate−water tetramer $R_4^4(12)$ ring motif.

dx.doi.org/10.1021/cg300002p | *Cryst. Growth Des.* 2012, 12, 2023−2036

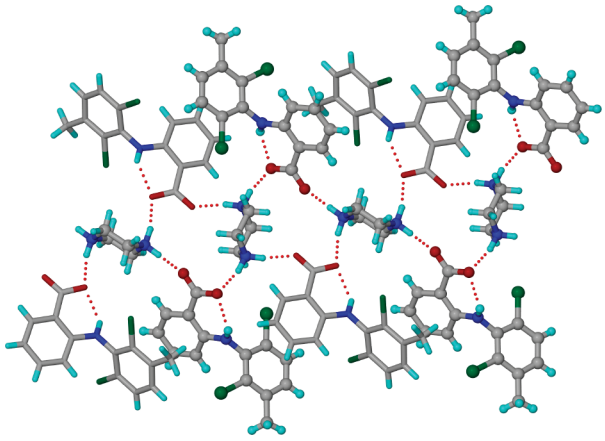

Figure 6. Two crystallographic molecules of meclofenamate (A = thick bond, B = ball-stick) and two half molecules of piperazine cations form $N^+-H\cdots O^-$ hydrogen bonds in the 2:1 salt of MFA–PPZ.

the stoichiometry as a monohydrate (calc. 4.68%, obsd. 4.71%). A mefenamic acid piperazine salt hydrate (2:1:4) was recently reported,[16] but its crystal structure is completely different from our results because of hydrogen bonding to four water molecules.

2-Aminopyridinium Meclofenamate Salt (1:1, MFA–2-APY). The organic cation and anion form $R_2^2(8)$ ring motif (Scheme 1) between amino-pyridinium and carboxylate via N–H···O bonds (N···O, 2.642(3) Å, 2.841(3) Å). Such dimer units are connected via amino N–H···O (N···O 2.897(3) Å) hydrogen bond (Figure 8a). The molecular packing extends via Cl···Cl type I interaction[17] (3.472(2) Å, $\theta_1 = \theta_2 = 135.8°$) and C–H···Cl interaction (H···Cl, 2.92(3) Å) in a zigzag chain along the *b*-axis (Figure 8b). Carboxylate C–O bond distances (1.252(3), 1.263(3) Å) and pyridinium ∠C–N–C bond angle (121.7(2)°) are consistent with a salt structure.

4-Aminopyridinium Meclofenamate Salt Hydrate (1:1:1, MFA–4-APY–H_2O). Proton transfer occurred from MFA to pyridine base in this salt hydrate. The expected carboxylate–pyridinium $R_2^2(7)$ ring motif is absent presumably due to stronger H bonds of carboxylate with water molecules. Two water molecules now make a dimeric $R_4^4(12)$ ring motif[12] capped with two carboxylates (Scheme 1) through O–H···O^- (O···O, 2.761(4) Å, 2.713(4) Å) hydrogen bonds. The 4-APY cation interacts with two water molecules through both ionic $N^+-H\cdots O$ (N···O, 2.837(4) Å) (Figure 9a) and neutral

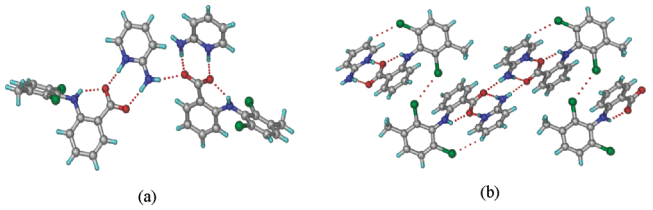

Figure 8. (a) Pyridine $(NH^+)\cdots{}^-OOC$ synthon in MFA–2-APY (conformer B of drug). (b) Cl···Cl and C–H···Cl interactions connect the molecules in a 1D wavelike chain.

N–H···O (N···O, 2.993 (4) Å) and one meclofenamate ion through N–H···O^- (N···O, 3.018 (4) Å) hydrogen bonds (Figure 9b). Water molecules are strongly hydrogen bonded in channels formed by MFA and 4-APY ions along the *c*-axis (Figure 9c). Carboxylate nature (C–O 1.261, 1.266 Å and ∠C–N–C 121.1°) and water stoichiometry by TGA (Figure S2, Supporting Information) were confirmed (calc 4.40%, obsd. 4.40%) in the monohydrate salt. Hydrogen bonding and unit cell parameters similarity of MFA–PPZ–H_2O and MFA–4-APY–H_2O (1:1:1) suggest 2D isostructurality and isomorphism, but there are differences in the 3D packing (Figure 7c vs 9c).

The conformation of MFA is different in crystal structures (Table 3). Both conformers A and B are well distributed in cocrystals/salts. A small contribution from an alternate conformation could be detected in a few cases (e.g., MFA–INA cocrystal) by the unassigned difference electron density (Q peaks of about 0.5–0.7 electron), but it was difficult to refine it as Me group occupancy. The small amount of Me group disorder in these structures is difficult to model accurately. The intramolecular N–H···O hydrogen bond locks the anthranilic acid fragment in a planar conformation, while the phenyl ring bearing the Cl and Me groups can rotate around the N–C bond. The formation of cocrystal or salt followed the ΔpK_a rule,[5] that is, $\Delta pK_a > 3$ gives salt, $\Delta pK_a < 0$ is for cocrystal, and the region $0 < \Delta pK_a < 3$ is a difficult to predict zone. The pK_a's (calculated using SPARC calculator in water medium) are listed in Table 4. The acid–acid dimer of MFA crystal structure is replaced by acid–pyridine heterosynthon in MFA–INA and MFA–BPY. Charge assisted $N^+-H\cdots O^-$ hydrogen bonds reproducibly give salts of MFA and piperazine/aminopyridine base. The N base inserts between the carboxylic acid groups to replace the carboxylic acid O–H···O homosynthon with the pyridinium/piperazinum–carboxylate charge assisted $N^+-H\cdots O^-$

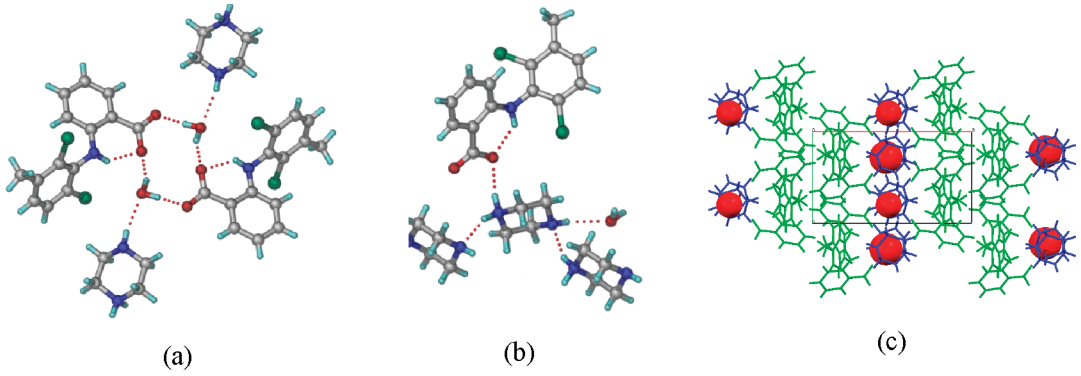

Figure 7. (a) Tetramer $R_4^4(12)$ ring motif between two meclofenamate anions and two water molecules in MFA–PPZ–H_2O (b) A piperazinium cation is surrounded by two similar cations, one water molecule, and one meclofenamate anion. (c) Water molecules are present in channels along the *c*-axis.

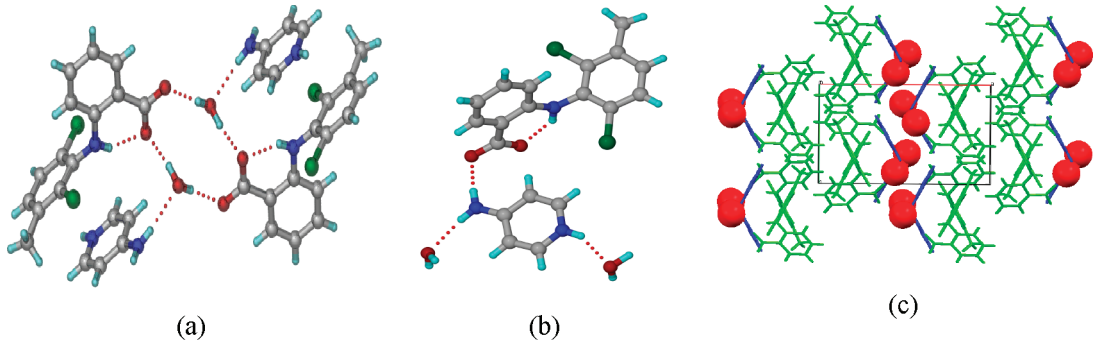

Figure 9. (a) Two meclofenamate anions (conformer A) and two water molecules form $R_4^4(12)$ ring through O−H···O$^-$ hydrogen bond in MFA−4-APY−H_2O. (b) 4-Aminopyridinium cation interacts with one meclofenamate anion and two water molecules through N−H···O$^-$ and N$^+$−H···O hydrogen bonds. (c) Water molecules reside in channels formed along the *c*-axis.

Table 3. Torsion Angles (°) in MFA Crystal Structures

	∠C2−C7−N1−C8 (deg)	∠C7−N1−C8−C9 (deg)	∠C7−N1−C8−C13 (deg)	∠C7−C2−C1−O1 (deg)	∠C7−C2−C1−O2 (deg)	conformer of MFA in crystal structure
MFA	173.46(2)	92.72(3)	86.44(3)	1.54(4)	177.71(2)	disorder
MFA−INA	163.21(2)	99.01(2)	81.84(2)	4.52(3)	174.63(2)	A
MFA−BPY	172.84(1)	86.50(1)	93.76(1)	3.71(2)	175.45(1)	A
MFA−PPZ-M	165.93(1)	98.87(1)	83.43(2)	4.20(2)	176.64(1)	B
MFA−PPZ-O	167.98(3)	66.12(4)	115.44(3)	0.16(4)	179.45(2)	A
MFA−PPZ	157.82(1), 161.44(1)	98.31(1), 84.42(1)	84.52(1), 95.47(1)	6.28(1), 14.42(1)	171.35(1), 165.67(1)	A + B
MFA−PPZ−H_2O	167.43(2)	108.04(3)	74.59(3)	8.59(3)	173.55(2)	B
MFA−2-APY	177.91(7)	71.22(11)	111.85(9)	6.49(11)	174.43(7)	B
MFA−4-APY−H_2O	171.60(4)	84.65(5)	98.50(5)	5.55(6)	176.02(4)	A

Table 4. Coformers Attempted to Make Cocrystal/Salts with MFA and ΔpK_a Values[a]

	pK_a/pK_b (water)	ΔpK_a	cocrystal/salt
meclofenamic acid	4.56		
isonicotinamide	4.17	0.39	1:1 cocrystal
4,4′-bipyridine	4.61	0.05	1:0.5 cocrystal
piperazine	9.72	5.16	1:1 salt polymorphs
piperazine	9.72	5.16	1:1:1 salt hydrate
piperazine	9.72	5.16	2:1 salt
2-amino pyridine	6.68	2.12	1:1 salt
4-amino pyridine	8.59	4.03	1:1:1 salt hydrate

[a] pK_a's were calculated in water using SPARC pK_a calculator, http://archemcalc.com/sparc/test/login.cfm?CFID=11677&CFTOKEN=94786654.

heterosynthon. This strong heterosynthon in MFA salts/cocrystals is a reliable tool for crystal engineering.

Powder X-ray Diffraction. Powder X-ray diffraction (PXRD)[18] is a reliable characterization technique to establish the formation of new solid materials. Rapid "fingerprinting" of the product phase (cocrystal/salt) compared to characteristic peaks in the starting materials (drug, coformer) is possible by eye-balling of the line patterns. PXRD of new materials prepared in this work (Figure S3, Supporting Information) confirms the purity and homogeneity of each crystalline phase by an excellent overlay of the experimental PXRD with the calculated lines from the crystal structure. Calculated PXRD line patterns of MFA−PPZ-M and MFA−PPZ-O salt polymorphs (prepared in mixed state) are compared in Figure S4, Supporting Information.

Thermal Analysis. A change in the melting point of cocrystal/salt in the DSC thermogram is usually indicative of a new phase. Any dissociation/decomposition and/or phase changes upon heating are indicated by endo-/exotherm in the DSC trace. The monoclinic and orthorhombic polymorphs of MFA−PPZ (1:1) melt at 162.6 and 145.8 °C suggesting that the high melting monoclinic form is more stable (Figure 10).

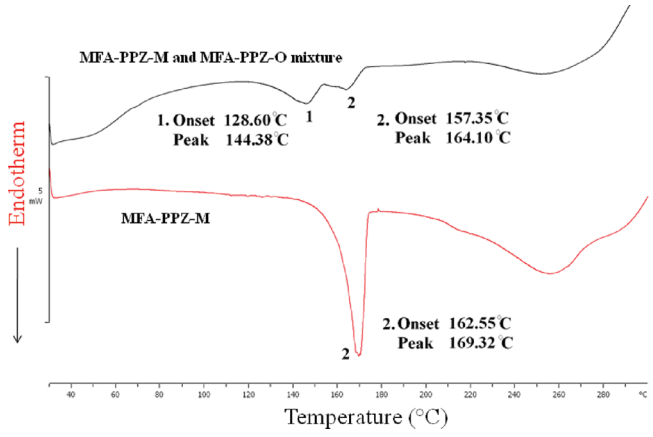

Figure 10. DSC endotherm comparisons for MFA−PPZ (1:1) salt polymorphs monoclinic (M) and orthorhombic (O).

The metastable orthorhombic form could not be reproduced in bulk scale purity. The DSC of polymorphic mixture (O + M) and pure monoclinic form are shown to compare their thermal behavior. Melting points are listed in Table 5. Dehydration of MFA−PPZ−H_2O resulted in an anhydrate that matched with the stable monoclinic form (MFA−PPZ-M). The dissociation of the cocrystal/salt to MFA above 240 °C is indicated by the broad endotherm after melting (see Figure S5, Supporting

dx.doi.org/10.1021/cg300002p | *Cryst. Growth Des.* 2012, 12, 2023−2036

Table 5. Melting Point of Cocrystal/Salt Compared with MFA and Coformers

	mp of MFA/ coformer (°C)	mp of cocrystal/salt (°C) (DSC, T_{onset})
MFA	257−260	
MFA−INA	155−158	176.8
MFA−BPY	110−114	207.1
MFA−PPZ-M	106−108	169.3
MFA−PPZ-O	106−108	144.4
MFA−PPZ−H_2O	106−108	97.3, 163.3
MFA−PPZ	106−108	171.9
MFA−2-APY	57−60	145.6
MFA−4-APY−H_2O	157−161	93.6, 111.7

Information). The dissociation of salts/cocrystals to MFA is similar to that for Diclofenac.[21e]

FT-IR and FT-Raman Spectroscopy. Spectroscopic analysis (IR and Raman)[19] showed clear differences in hydrogen bonding of salt/cocrystal compared to the pure components. Such peak shifts are useful to know specific functional groups which are involved in intermolecular interactions. Generally speaking, for fenamic acids,[19b] NH stretch appears at 3300−3350 cm^{-1}. The band at about 3335 cm^{-1} arises from the amino group internally hydrogen bonded to the C═O of MFA. Carboxylic acid C═O stretch is normally at 1700−1720 cm^{-1}, but due to intramolecular hydrogen bonds in MFA the C═O stretch is red-shifted at 1655 cm^{-1}. Bands due to C−O stretch and O−H bend appear at 1256 cm^{-1} and 1400 cm^{-1}. The carboxylate anion in salts showed two bands, a strong asymmetric stretch at 1650−1550 cm^{-1}, and a weaker symmetric stretch near 1450 cm^{-1}. FT-IR and FT−Raman frequencies are summarized in Tables 6 and 7.

Solid State NMR Spectroscopy. ss-NMR spectroscopy[20] of MFA−PPZ (1:1), MFA−PPZ monohydrate (1:1:1), and MFA−PPZ (2:1) was informative about local short-range order in these solid-state structures (Figure 11, Table S3). Two peaks at δ 18.34 and 20.06 ppm represent the methyl group of MFA which is disordered over two positions. The chemical shifts in the NMR spectra of MFA−PPZ-M (1:1) and MFA−PPZ−H_2O (1:1:1) salts are similar because the same conformer B of MFA is present in both structures. There is an extra ^{13}C peak in MFA−PPZ (2:1) for piperazinium cation at δ 37.33 ppm, methyl carbon at 21.23 ppm, and carboxylate peak at δ 175.07 ppm, consistent with the crystal structure which showed two MFA conformers A and B and two nonequivalent piperazinium cations. The downfield region peaks in the ss-NMR spectrum of salts (COO^-) are shifted relative to the free acid (COOH).

Solution Mediated Phase Transformations. Solution mediated phase transformations[21] are common in pharmaceuticals, that is, the transformation of one phase to another in a suspension or slurry medium. Such phase changes can also occur upon wet granulation and thus need to be monitored in dosage formulation. 50% EtOH−water solvent was used because the drug and cocrystals/salts are soluble in this medium. The same solvent system was used for solubility and dissolution experiments (discussed next). Piperazinium meclofenamate (1:1) and (1:1:1) salt hydrate converted to piperazinium meclofenamate (2:1) after 24 h slurry in 50% EtOH−water at 37 °C (Figures 12 and 13). The product 2:1 salt converted to MFA after another 24 h in the same slurry medium (Figure 14). Fini et al.[21e] reported 1:1 and 2:1 salts of diclofenac-pirperazine while our work was in review. Their 1:1 salt transforms to the less soluble 2:1 salt after one week in distilled water during slurry experiments, similar to our results. We surmise that the more soluble coformer piperazine dissociates from the salt in the aqueous medium and the less soluble drug MFA precipitates after 48 h. The dissociation of piperazine from the salt occurs in stages: half equivalent in 24 h (1:1 to 2:1 salt), and then another half equivalent in next 24 h (to give MFA) as confirmed by PXRD of the solid residue. The stability of

Table 6. FT-IR Stretching Modes (ν_s, cm^{-1}) of MFA and Its Cocrystals/Salts[a]

	N−H stretch	C═O stretch	N−H bend	C−O stretch (asym)	C−O stretch (sym)
MFA	3335.1	1655.4	1575.3	1437.4	1256.6
MFA−INA	3447.0, 3227.2	1694.8	1559.5	1449.5	1261.5
MFA−BPY	3245.9	1675.4	1600.4, 1581.4	1451.0	1259.7
MFA−PPZ-M	3216.9		1582.4	1452.9	1289.1
MFA−PPZ−H_2O	3208.4, 3172.6		1576.4	1452.1	1282.5
MFA−PPZ	3497.3, 3267.0		1577.8	1452.5	1287.6
MFA−2-APY	3268.5, 3199.8		1577.7	1449.1, 1458.1	1288.1, 1255.0
MFA−4-APY−H_2O	3436.7, 3346.2, 3301.2		1574.7	1455.2	1288.0

[a]IR spectrum of MFA−PPZ-O salt could not be recorded due to insufficient sample and contamination from the stable monoclinic polymorph in the bulk phase.

Table 7. FT-Raman Stretching Modes (ν_s, cm^{-1}) of MFA and Its Cocrystal/Salts[a]

	C−H stretch	C═O stretch	N−H bend	C−O stretch (asymm)	C−O stretch (sym)
MFA	3079.6, 2925.2	1655.2	1577.5	1439.1	1242.3
MFA−INA	3071.4	1675.0	1602.1	1449.2	1243.2
MFA−BPY	3086.9, 3053.6	1663.2	1582.3	1450.8	1239.8
MFA−PPZ-M	3070.8, 2983.6		1580.1	1448.4	1271.6
MFA−PPZ−H_2O	3079.2, 3002.6		1581.1	1450.2	1274.4
MFA−PPZ	3070.1, 2973.4		1582.5	1445.5	1281.0
MFA−2-APY	3073.5, 2924.5		1579.4	1448.4	1273.2
MFA−4-APY−H_2O	3059.7, 2924.4		1573.7	1453.4	1267.1

[a]Raman spectrum of MFA−PPZ-O salt could not be recorded due to insufficient sample and contamination from the stable monoclinic polymorph in the bulk phase.

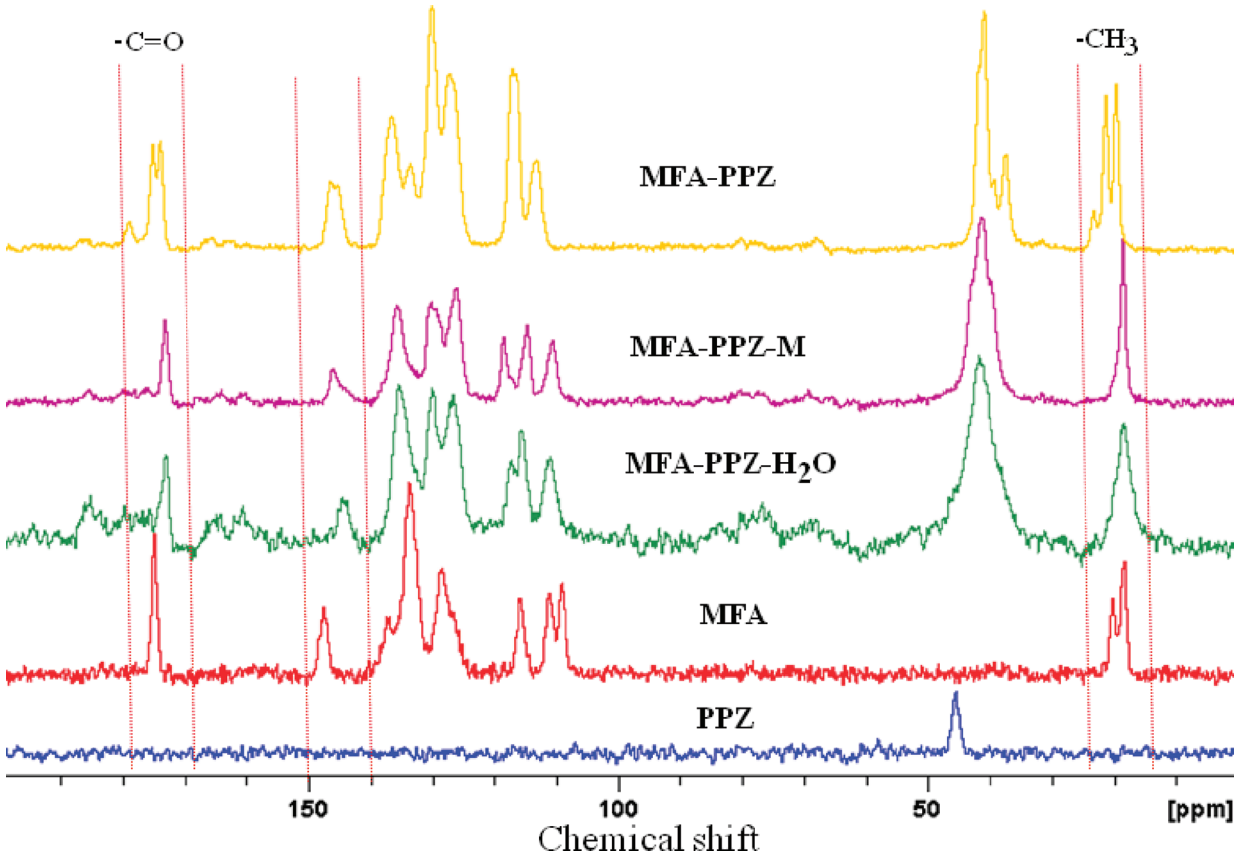

Figure 11. Solid state ^{13}C NMR spectra of MFA−PPZ-M (1:1, pink) and MFA−PPZ−H_2O (1:1:1, green) and MFA−PPZ (2:1, yellow) salts along with the pure components. The peaks in the salt are shifted relative to the pure components because of carboxylic acid to carboxylate in MFA. The regions of main chemical shift differences are indicated in red line border.

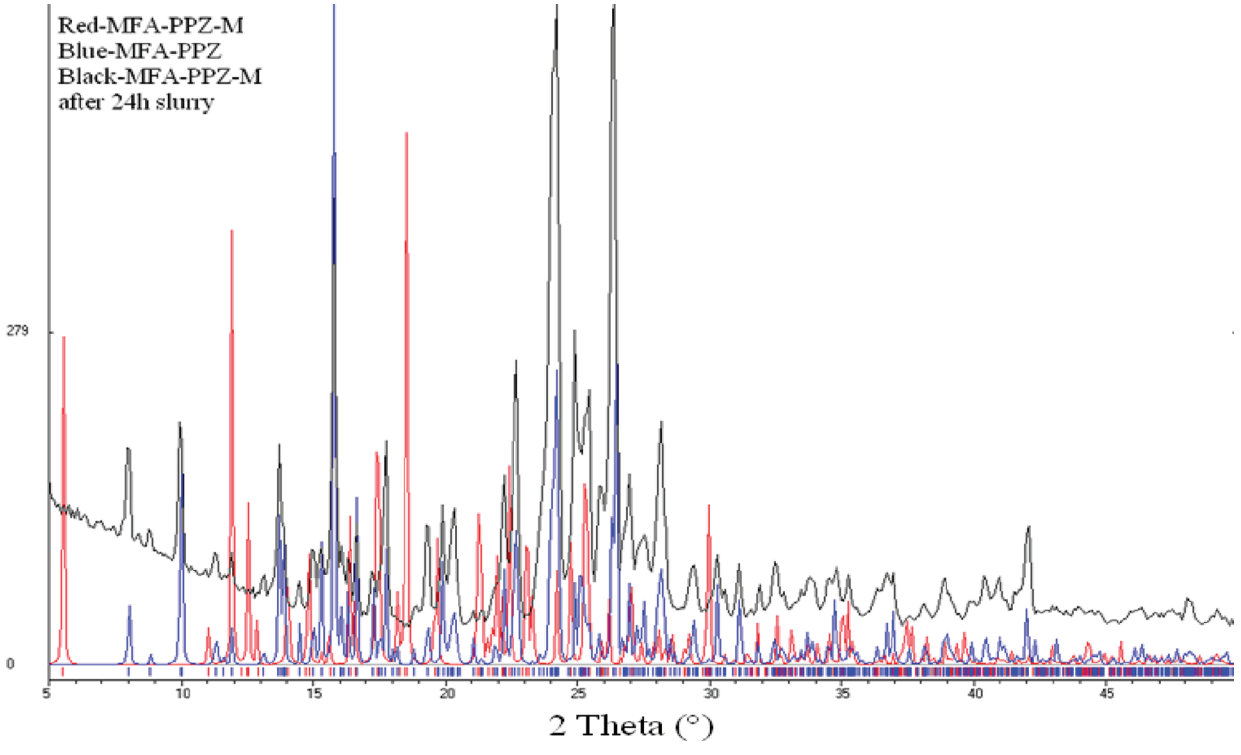

Figure 12. PXRD comparison of MFA−PPZ-M (black) after 24 h slurry with the calculated X-ray lines of MFA−PPZ-M (red) and MFA−PPZ 2:1 salt (blue) in 50% EtOH−water medium. The monoclinic polymorph undergoes solvent mediated phase transformation from MFA−PPZ-M to MFA−PPZ salt after 24 h.

dx.doi.org/10.1021/cg300002p | *Cryst. Growth Des.* 2012, 12, 2023−2036

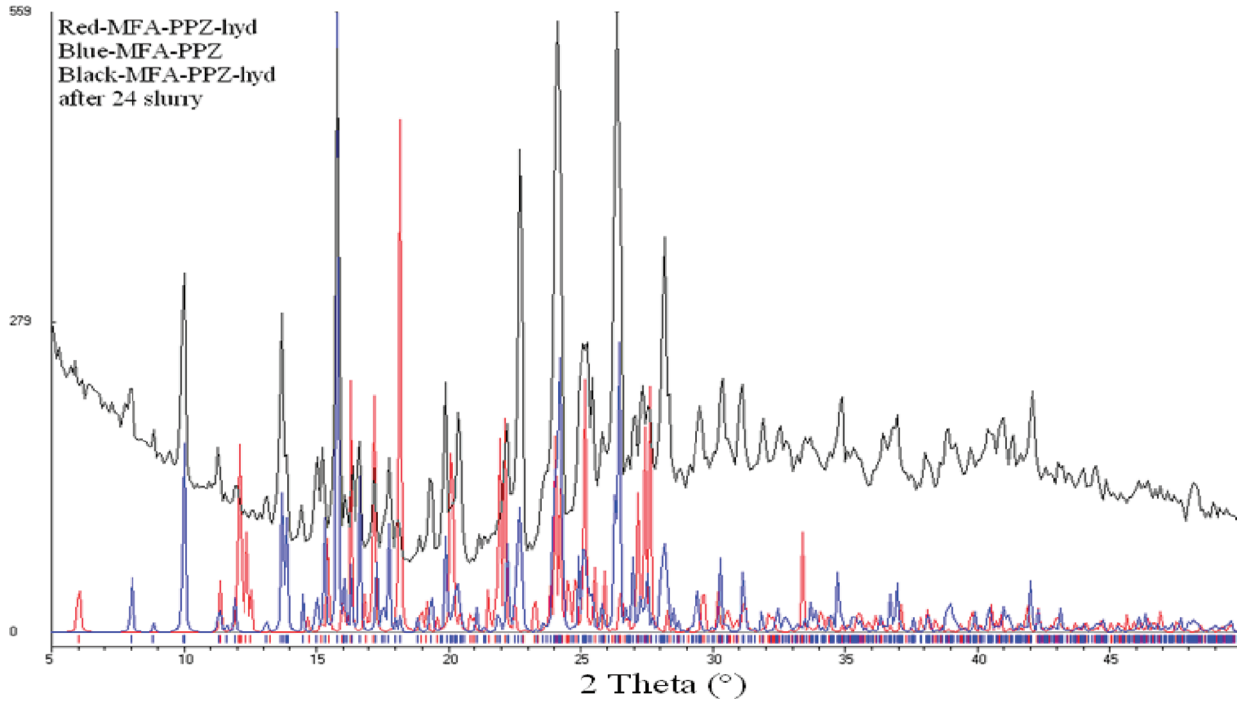

Figure 13. PXRD comparison of MFA−PPZ−H_2O (black) after 24 h slurry with the calculated X-ray lines of MFA−PPZ−H_2O (red) and MFA−PPZ 2:1 (blue) in 50% EtOH−water medium. The hydrate MFA−PPZ−H_2O transforms to MFA−PPZ salt after 24 h.

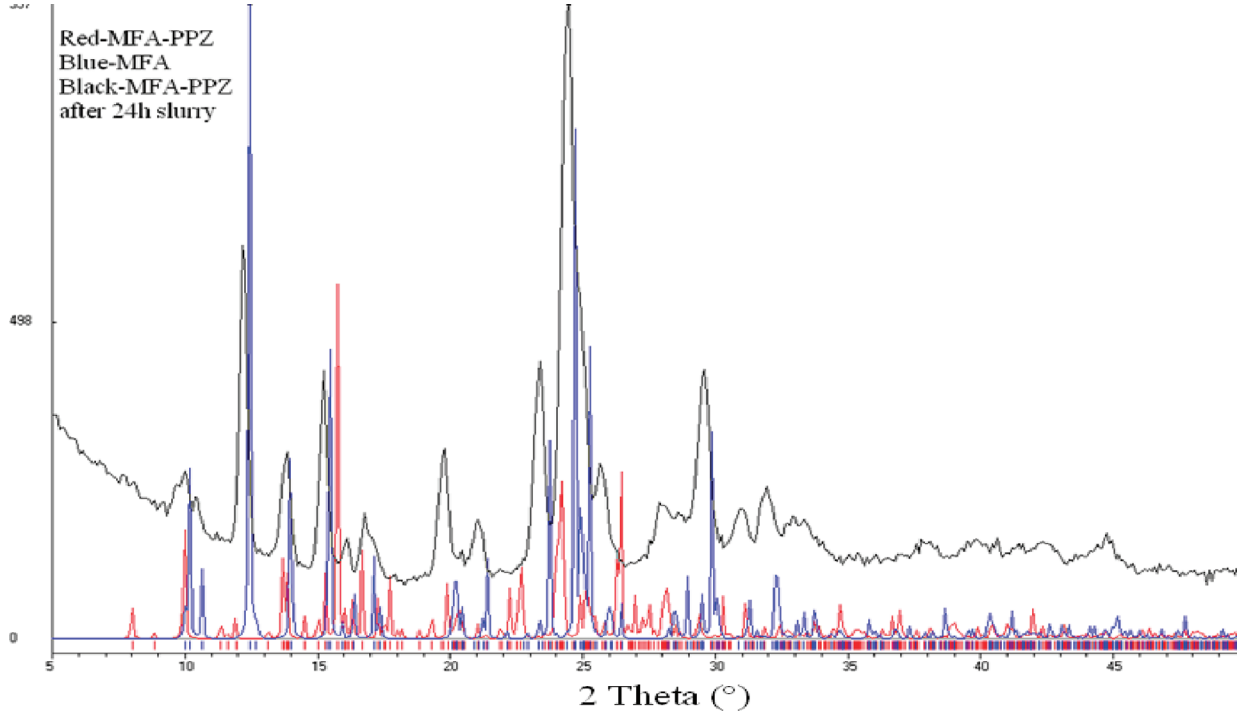

Figure 14. PXRD comparison of MFA−PPZ 2:1 (black) after 24 h slurry with the calculated X-ray lines of MFA−PPZ 2:1 (red) and MFA (blue) in 50% EtOH−water medium. MFA−PPZ 2:1 salt transforms to pure MFA after 24 h.

variable stoichiometry salts in slurry medium may be related to their hydrogen bonding in the crystal structures: the 1:1 salt contains one N^+−H···O^- and one N−H···O hydrogen bond between meclofenamate and piperazinium, whereas one meclofenamate interacts with a dipiperazinium through two N^+−H···O^- hydrogen bonds in the 2:1 salt. The stronger ionic H bonds result in greater stability of the 2:1 salt over the 1:1 salt. MFA−PPZ monohydrate (1:1:1) showed similar results. The cocrystals, on the other hand, were more stable to slurry conditions: MFA−INA transformed to 86% MFA and 14% cocrystal remained after 24 h, as confirmed by PXRD. A calibration sample of 85% MFA and 15% cocrystal suggested that the standard deviation of PXRD is ±3%. MFA−BPY cocrystal was unusually stable for up to 72 h in 50% EtOH−water medium (Figure S6, Supporting Information). These stability trends may be ascribed to congruent and incongruent

dx.doi.org/10.1021/cg300002p | *Cryst. Growth Des.* 2012, 12, 2023−2036

systems.[22] When the solubility of the drug and the coformer are similar in the same medium (both are insoluble/less soluble), such systems are congruent and tend to be stable. For incongruent systems, the high solubility coformer leaches into the solvent medium in which it readily dissolves, and in this way the salt/cocrystal dissociates faster. The soluble cocrystals will usually have a highly soluble coformer partner and this in turn makes the salt/cocrystal of limited stability. This in effect puts a limit to the stability of more soluble pharmaceutical cocrystals in the slurry medium. The stability order in aqueous slurry medium is (less to more stable): MFA−PPZ (1:1) < MFA−PPZ monohydrate (1:1:1) < MFA−PPZ (2:1) < MFA−INA (1:1) < MFA−BPY (1:0.5). Solution-mediated phase transformations[21] can occur during dissolution and solubility measurements (discussed next), and the above stability order will help to explain any unusual trends.

Solubility and Dissolution Experiments. The rate of dissolution and solubility of the solid drug in water or aqueous solvent mixtures is necessary for good oral bioavailability. The aqueous solubility of the drug must be at least 100 mg/L for fast dissolution of the tablet.[1c] The aqueous solubility of MFA is 30 mg/L and other fenamic acids (e.g., mefenamic acid, tolfenamic acid and diclofenamic acid) are also low solubility BCS class II drugs. The sodium salt of meclofenamic acid (MFA-SS) is marketed as capsules (solubility > 250 g/L). The aqueous solubility for cocrystals and salts of MFA were measured in 50% EtOH−water medium at 37 °C (Table 8).

Table 8. Solubility and Dissolution Rate of MFA and Its Cocrystals and Salts[a]

solid form	absorption coefficient (ε, mM^{-1} cm^{-1})	equilibrium solubility after 24 h slurry in 50% EtOH−water (mg L^{-1})	IDR ((mg cm^{-2}) min^{-1})[a]
MFA	6.94	203.11	0.03074
MFA−INA	4.10	581.43 (x 2.9)	0.04858 (x 1.6)
MFA−BPY	5.74	1638.07 (x 7.6)	0.03822 (x 1.2)
MFA−PPZ-M	3.38	553223.061 (x 2724)	27.4976 (x 894.5)
MFA−PPZ	7.95	10211.954 (x 50)	0.31477 (x 10.2)
MFA−PPZ−H_2O	4.82	270966.397 (x 1334)	9.8044 (x 318.9)

[a]Number in parentheses indicates how many times higher solubility/IDR compared to reference drug.

Although solubility is a good indicator of drug bioavailability, the method is applicable only for those solid-state drug forms which are stable in the test medium/wet slurry. The intrinsic dissolution rate (IDR) is a kinetic parameter and is a useful indicator for those solid forms which undergo phase transformation or dissociation during the experiment. Most drugs exert their therapeutic effect during 4−6−8 h of oral administration, and IDR is related to drug dissolution in such cases. IDR measurements showed that piperazine salts reached peak concentration within 30−45 min of drug dissolution (Figure 15). The most stable 2:1 MFA−PPZ salt exhibited a gradual increase in dissolution rate up to 24 h. The cumulative amount of MFA dissolved (mg cm^{-2}) vs time (min) was plotted to compare the IDR of piperazine meclofenamates (Figure 15a). The highest solubility of MFA−PPZ-M (1:1) is driven by the high solubility of piperazine > MFA−PPZ−H_2O (1:1:1) because hydrates are generally less soluble than anhydrate drugs > (MFA−PPZ (2:1) due to lower piperazine content. In contrast to salts, MFA−INA (1:1) and MFA−BPY (1:0.5) cocrystals exhibited poor dissolution rates (Figure 15b), but they were

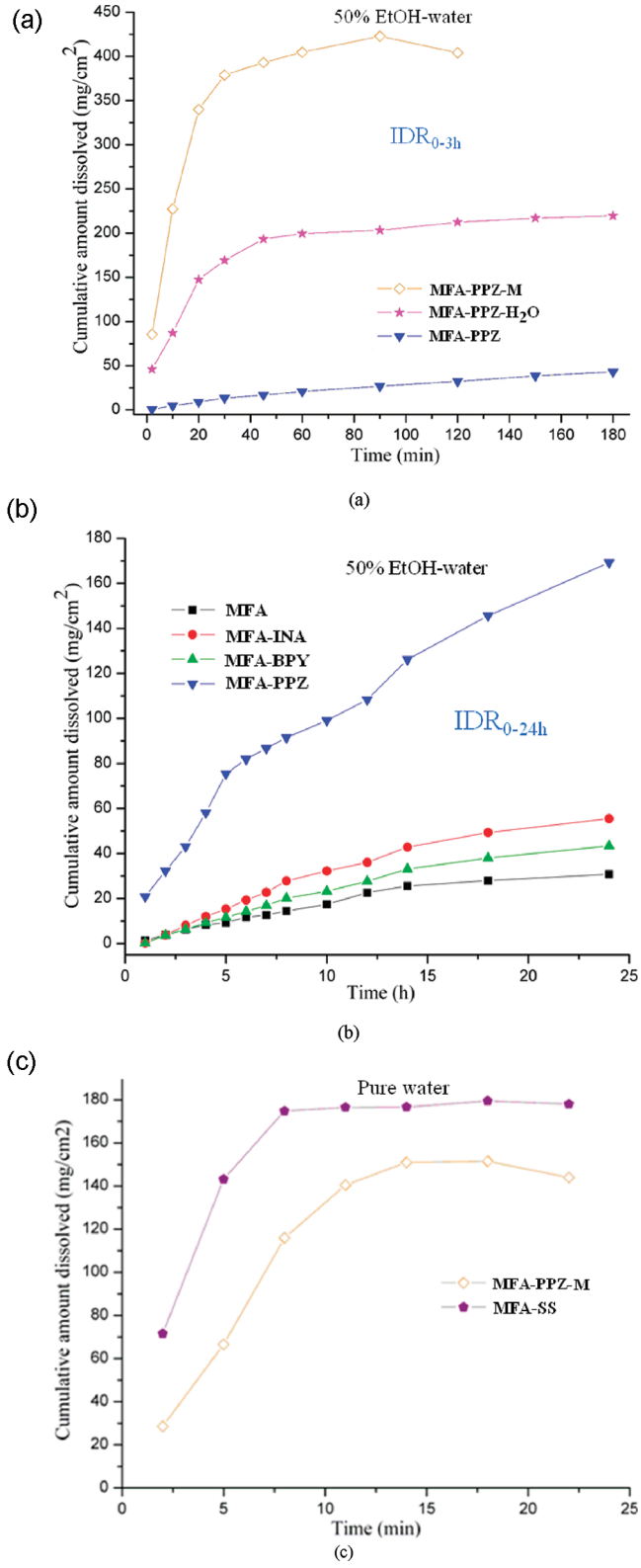

Figure 15. Intrinsic dissolution rate (IDR) measurements of (a) MFA−PPZ-M (1:1), MFA−PPZ−H_2O (1:1:1) and MFA−PPZ (2:1) performed up to 3 h, (b) MFA−PPZ (2:1), MFA−INA (1:1), MFA−BPY (1:0.5) and MFA over 24 h in 50% EtOH−water medium, and (c) MFA−PPZ-M (1:1) and MFA-SS (sodium salt of MFA) over 22 min in distilled water. The amount of MFA dissolved in the test medium was monitored by UV−vis spectroscopy.

quite stable for over 24 h (Figure S6, Supporting Information). The highest solubility salt MFA−PPZ (1:1) was compared

dx.doi.org/10.1021/cg300002p | Cryst. Growth Des. 2012, 12, 2023−2036

with MFA-SS in aqueous medium; IDR of sodium salt is 28.76 and piperazinium salt is 13.72 (mg cm^{-2}) min^{-1} (Figure 15c). The marketed sodium salt of MFA has 2.1 times higher IDR than the equimolar piperazine salt. PXRD of the residue of MFA−PPZ-M dissolution experiment after 11 min matched with the 2:1 salt (70%) and monohydrate (30%), the 1:1 salt showed transformation to piperazine salt hydrate and 2:1 salt, whereas the MFA sodium salt transformed to its hydrate after 8 min in the dissolution medium. These results suggest that 1:1 MFA−PPZ-M is more stable than the marketed sodium salt to hydration in aqueous medium. PXRD of melofenamic acid sodium salt after 24 h of slurry stirring in water (Figure S7, Supporting Information) is different from the starting material (MFA-SS, Sigma-Aldrich). Thermogravemetric analysis and Karl Fischer titration method indicate a water content of 13.92% (2.8−2.9 equivalent) in MFA-SS hydrate (Figure S8, Supporting Information) formed in the aqueous medium, a value that was confirmed by DSC. The aqueous solubility of sodium salt of MFA (>250 g/L)[7b] is 46 times greater than the value for MFA−PPZ-M 1:1 salt in water (5.4 g/L), but its dissolution rate is two times faster in the first 30 min of measurement.

■ CONCLUSIONS

MFA is the most potent nonsteroidal anti-inflammatory drug. A few cocrystals and salts of MFAs were crystallized using crystal engineering principles. All new crystalline phases were characterized by X-ray diffraction, IR and ss-NMR spectroscopy, and DSC/TGA. MFA exists in two different conformers A and B due to m-tolyl group rotation about the N−C bond. Whereas the crystal structure of MFA has disordered methyl groups, the drug molecule is in an ordered orientation in its cocrystals and salts, perhaps rigidified due to stronger hydrogen bonding. The dissolution rate and solubility of MFA−PPZ-M 1:1 salt is the highest among the novel solid-state forms studied and slightly lower than the marketed sodium salt of MFA. Their stability to hydration is comparable in aqueous medium. Thus, meclofenamate piperazinium has an equivalent dissolution and stability profile to the marketed sodium salt. Four different piperazinium salts were crystallized: monoclinic and orthorhombic polymorphs of MFA−PPZ (1:1), its monohydrate, and MFA−PPZ (2:1). This is the first example of polymorphic and variable stoichiometry piperazinium salts with X-ray crystal structures solved to good accuracy.

■ EXPERIMENTAL SECTION

MFA and INA were purchased from Sigma-Aldrich (Hyderabad, Andhra Pradesh, India) and used directly for experiments. All other chemicals were of analytical or chromatographic grade. Melting points were measured on a Fisher-Johns melting point apparatus. Water filtered through a double deionized purification system (AquaDM, Bhanu, Hyderabad, India) was used in all experiments. Single crystals were obtained via slow evaporation of stoichiometric amounts of starting materials in an appropriate solvent. Cocrystals and salts were characterized by infrared spectroscopy (IR), powder X-ray diffraction (PXRD), differential scanning calorimetry (DSC), thermogravimetric analysis (TGA), and single crystal X-ray diffraction (SC-XRD).

Meclofenamic Acid, MFA. Normally cracked crystals of MFA appeared after crystallization from organic solvents. Sublimation of MFA at 190−200 °C produced good quality block shaped crystal after 2−3 h. Melting point 257−260 °C (literature value).[7a,23]

Meclofenamic Acid−Isonicotinamide, MFA−INA (1:1) Cocrystal. MFA (100 mg, 0.34 mmol) and INA (41.5 mg, 0.34 mmol) were ground in a mortar pestle for 15 min using acetonitrile as solvent-assisted grinding. After a new solid phase was confirmed by IR and PXRD, the bulk material was dissolved in acetonitrile. Good quality single crystals appeared at ambient conditions after 2−3 days, mp 175−177 °C.

Meclofenamic Acid−4,4′-Bipyridine, MFA−BPY (1:0.5) Cocrystal. MFA (100 mg, 0.34 mmol) and BPY (26.5 mg, 0.17 mmol) were ground in a mortar pestle for 15 min using acetonitrile as solvent-assisted grinding. After a new solid phase was confirmed by IR and PXRD, the bulk material was dissolved in acetonitrile. Thick plate crystals were harvested at ambient conditions after 2−3 days, mp 204−207 °C.

Piperazinium Meclofenamate, MFA−PPZ (1:1) Salt Polymorphs. MFA (100 mg, 0.34 mmol) and piperazine (29.3 mg, 0.34 mmol) were ground in a mortar pestle for 15 min using acetonitrile as solvent-assisted grinding. After a new solid phase was confirmed by IR and PXRD, the bulk material was dissolved in acetonitrile. Block (monoclinic, form M) and thick long needle (orthorhombic, form O) crystals were harvested concomitantly at ambient conditions after 2−3 days. Monoclinic form (plate) was obtained exclusively from CH_3NO_2 solvent; mp of monoclinic and orthorhombic forms are 162−166 °C and 144−147 °C, respectively.

Piperazinium Meclofenamate, MFA−PPZ (2:1) Salt. MFA (100 mg, 0.34 mmol) and piperazine (29.3 mg, 0.34 mmol) were ground in a mortar pestle for 15 min using acetonitrile as solvent-assisted grinding. After a new solid phase was confirmed IR and PXRD, bulk material was dissolved in EtOH. Suitable thick plate (triclinic) crystals were harvested at room temperature after 3−4 days, mp 166−169 °C.

Piperazinium Meclofenamate Monohydrate, MFA−PPZ−H_2O (1:1:1) Salt. MFA (100 mg, 0.34 mmol) and piperazine hydrate (35.4 mg, 0.34 mmol) were ground in a mortar pestle for 15 min After a new solid phase was confirmed by IR and PXRD, the bulk material was dissolved in nitromethane, mp of salt 154−158 °C and dehydration temperature 92−95 °C.

2-Aminopyridinium Meclofenamate, MFA−2-APY (1:1) Salt. MFA (100 mg, 0.34 mmol) and 2-aminopyridine (32 mg, 0.34 mmol) were ground in a mortar pestle for 15 min using acetonitrile as solvent-assisted grinding. After a new solid phase was confirmed by IR and PXRD, the bulk material was dissolved in acetonitrile. Plate crystals were harvested after 2−3 days at ambient condition, mp 143−146 °C.

4-Aminopyridinium Meclofenamate Monohydrate, MFA−4-APY−H_2O (1:1:1) Salt. MFA (100 mg, 0.34 mmol) and 4-aminopyridine (32 mg, 0.34 mmol) were ground in a mortar pestle for 15 min using acetonitrile as solvent-assisted grinding. After a new solid phase was confirmed by IR and PXRD, bulk material was dissolved in acetonitrile. Suitable thick plate crystals were harvested after 2−3 days at ambient condition, mp 104−108 °C and dehydration temperature 80−84 °C.

Single Crystal X-ray Diffraction. A single crystal obtained from the crystallization solvent(s) was mounted on the goniometer of Oxford CCD X-ray diffractometer (Yarnton, Oxford, UK) equipped with Mo−Kα radiation (λ = 0.71073 Å) source. Data reduction was performed using CrysAlisPro 171.33.55 software.[24] Crystal structures were solved and refined using Olex2−1.0[25] with anisotropic displacement parameters for non-H atoms. Hydrogen atoms were experimentally located through the Fourier difference electron density maps in all crystal structures. All O−H, N−H, and C−H atoms were geometrically fixed using HFIX command in SHELX-TL program of Bruker-AXS.[26] A check of the final cif file with PLATON[27] did not show any missed symmetry. X-Seed[28] was used to prepare the figures and packing diagrams. Crystallographic parameters of both structures are summarized in Table 1. Hydrogen bond distances in Table 2 are neutron-normalized to fix the D−H distance to its accurate neutron value in the X-ray crystal structures (O−H 0.983 Å, N−H 0.82 Å, C−H 1.083 Å). Crystallographic .cif files (CCDC Nos. 859220−859229) are available at www.ccdc.cam.ac.uk/data_request/cif or as part of the Supporting Information.

Powder X-ray Diffraction. Bulk samples were analyzed by PXRD on a Bruker AXS D8 diffractometer (Bruker-AXS, Karlsruhe, Germany). Experimental conditions: Cu−Kα radiation (λ = 1.54056 Å); 40 kV; 30 mA; scanning interval 5−50° 2θ at a scan rate of 1° min^{-1}; time per step 0.5 s. The experimental PXRD patterns and

calculated X-ray lines from the single crystal structure were compared to confirm the purity of the bulk phase using Powder Cell.[29]

Thermal Analysis. DSC and TGA were performed on a Mettler Toledo DSC 822e module and a Mettler Toledo TGA/SDTA 851e module, respectively. Samples were placed in open alumina pans for TGA and in crimped but vented aluminum sample pans for DSC. A typical sample size is 4−6 mg for DSC and 9−12 mg for TGA. The temperature range was 30−250 °C at 2 K min^{-1} for DSC and 10 K min^{-1} for TGA. Samples were purged with a stream of dry N_2 flowing at 150 mL min^{-1} for DSC and 50 mL min^{-1} for TGA.

Vibrational Spectroscopy. A Thermo-Nicolet 6700 FT-IR spectrometer (Waltham, MA, USA) with a NXR FT-Raman Module (Nd:YAG laser source, 1064 nm wavelength) was used to record IR and Raman spectra. IR spectra were recorded on samples dispersed in KBr pellets. Raman spectra were recorded on samples contained in standard NMR diameter tubes or on compressed samples contained in a gold-coated sample holder.

Solid-State NMR Spectroscopy. Solid-state ^{13}C NMR (ss-NMR) spectroscopy provides structural information about differences in hydrogen bonding, molecular conformations, and molecular mobility in the solid state. The solid-state ^{13}C NMR spectra were obtained on a Bruker Ultrashield 400 spectrometer (Bruker BioSpin, Karlsruhe, Germany) utilizing a ^{13}C resonant frequency of 100 MHz (magnetic field strength of 9.39 T). Approximately 100 mg of crystalline sample was lightly packed into a zirconium rotor with a Kel-F cap. The cross-polarization, magic angle spinning (CP-MAS) pulse sequence was used for spectral acquisition. Each sample was spun at a frequency of 5.0 ± 0.01 kHz and the magic angle setting was calibrated by the KBr method. Each data set was subjected to a 5.0 Hz line broadening factor and subsequently Fourier transformed and phase corrected to produce a frequency domain spectrum. The chemical shifts were referenced to TMS using glycine ($\delta_{glycine}$ = 43.3 ppm) as an external secondary standard.

Dissolution and Solubility Measurements. Intrinsic dissolution rate (IDR) and solubility measurements were carried out on a USP-certified Electrolab TDT-08 L Dissolution Tester (Electrolab, Mumbai, MH, India). A calibration curve was obtained for all the new solid phases including MFA by plotting absorbance vs concentration UV−vis spectra curves on a Thermo Scientific Evolution EV300 UV−vis spectrometer (Waltham, MA, USA) for known concentration solutions in 50% EtOH−water medium. The mixed solvent system (EtOH−water) was selected for its higher solubility of MFA in this medium. The slope of the plot from the standard curve gave the molar extinction coefficient (ε) by applying the Beer−Lambert's law. Equilibrium solubility was determined in 50% EtOH−water medium using the shake-flask method.[27] To obtain the equilibrium solubility, 100 mg of each solid material was stirred for 24 h in 5 mL of 50% EtOH−water at 37 °C, and the absorbance was measured at 318 nm. The concentration of the saturated solution was calculated at 24 h, which is referred to as the equilibrium solubility of the stable solid form.

100 mg of the solid (drug, cocrystal, salt) was taken in the intrinsic attachment and compressed to a 0.5 cm^2 pellet using a hydraulic press at a pressure of 2.5 ton/$inch^2$ for 2 min. The pellet was compressed to provide a flat surface on one side and the other side was sealed. Then the pellet was dipped into 900 mL of 50% EtOH−water medium at 37 °C with the paddle rotating at 150 rpm. At a regular interval of 5−10 min, 5 mL of the dissolution medium was withdrawn and replaced by an equal volume of fresh medium to maintain a constant volume. Samples were filtered through 0.2 μm nylon filter and assayed for drug content spectrophotometrically at 318 nm on a Thermo-Nicolet EV300 UV−vis spectrometer. There was no interference to MFA UV−vis maxima at 318 nm by coformers INA and bipyridine which absorb strongly at 250−270 nm. Piperazine is UV−vis inactive. The amount of drug dissolved in each time interval was calculated using the calibration curve. The linear region of the dissolution profile was used to determine the intrinsic dissolution rate (IDR) of the compound (= slope of the curve, that is, the amount of drug dissolved divided by the surface area of the disk (0.5 cm^2) per minute). The dissolution rates for MFA, its cocrystals, and salts were computed from their IDR values. Similarly IDR experiments of MFA−PPZ-M and MFA-SS salts were carried out in distilled water and absorbance was measured at 318 nm in a UV−vis spectrophotometer.

■ ASSOCIATED CONTENT

Supporting Information

Crystallographic information files; Refcodes of cocrystals and salts of piperazine (Table S1) and piperazinium dications with carboxylate anions (Table S2); ^{13}C solid-state NMR of piperazinium meclofenamate salts compared to values for the pure coformers (Table S3); ORTEP diagrams (Figure S1); TGA results (Figure S2); PXRD results (Figures S3, S6, S7); comparison of calculated X-ray diffraction lines of monoclinic and orthorhombic forms of piperazinium meclofenamate (1:1) salts (Figure S4); DSC endotherm (Figure S5); DSC and TGA thermograms (Figure S8). This material is available free of charge via the Internet at http://pubs.acs.org.

■ AUTHOR INFORMATION

Corresponding Author

*E-mail: ashwini.nangia@gmail.com.

Notes

The authors declare no competing financial interest.

■ ACKNOWLEDGMENTS

We thank the DST (SR/S1/OC-67/2006), JC Bose fellowship (SR/S2/JCB-06/2009), and CSIR (01(2410)/10/EMR-II) for research funding, and DST (IRPHA) and UGC (PURSE grant) for providing instrumentation and infrastructure facilities. P.S. and G.B. thank the UGC for fellowship. We thank Dr. Naba Kamal Nath for his assistance to resolve disorder issues in crystal structure refinement of MFA.

■ REFERENCES

(1) (a) Lipinski, C. *Am. Pharm. Rev.* **2002**, *5*, 82. (b) Vippagunta, S. R.; Brittain, H. G.; Grant, D. J. W. *Adv. Drug Delivery Rev.* **2001**, *48*, 3. (c) Byrn, S. R.; Pfeiffer, R. R.; Stowell, J. G. *Solid-State Chemistry of Drugs*, 2nd ed.; SSCI, Inc.: West Lafayette, IN, 1999.

(2) (a) Desiraju, G. R. *Crystal Engineering: The Design of Organic Solids*; Elsevier: Amsterdam, 1989. (b) Desiraju, G. R. *Angew. Chem., Int. Ed.* **2007**, *46*, 8342. (c) Blagden, N.; Matas, M. D.; Gavan, P. T.; York., P. *Adv. Drug Delivery Rev.* **2007**, *59*, 617.

(3) (a) Karki, S.; Friščić, T.; Fábián, L.; Laity, P. R.; Day, G. M.; Jones, W. *Adv. Mater.* **2009**, *21*, 3905. (b) Childs, S. L.; Chyall, L. J.; Dunlap, J. T.; Smolenskaya, V. N.; Stahly, B. C.; Stahly, G. P. *J. Am. Chem. Soc.* **2004**, *126*, 13335. (c) Remenar, J. F.; Morissette, S. L.; Peterson, M. L.; Moulton, B.; MacPhee, J. M.; Guzmán, H. R.; Almarsson, Ö *J. Am. Chem. Soc.* **2003**, *125*, 8456. (d) Cheney, M. L.; Shan, N.; Healey, E. R.; Hanna, M.; Wojtas, L.; Zaworotko, M. J.; Sava, V.; Song, S.; Sanchez-Ramos, J. R. *Cryst. Growth Des.* **2010**, *10*, 395. (e) Sanphui, P.; Goud, N. R.; Khandavilli, U. B. R.; Nangia, A. *Cryst. Growth Des.* **2011**, *11*, 4135.

(4) (a) Portell, A.; Barbas, R.; Font-Bardia, M.; Dalmases, P.; Prohens, R.; Puigjaner, C. *CrystEngComm* **2009**, *11*, 791. (b) Thakuria, R.; Nangia, A. *CrystEngComm* **2011**, *13*, 1759. (c) Banerjee, R.; Bhatt, P. M.; Ravindra, N. V.; Desiraju, G. R. *Cryst. Growth Des.* **2005**, *5*, 2299.

(5) (a) Aakeröy, C. B.; Fasulo, M. E.; Desper, J. *Mol. Pharmaceutics* **2007**, *4*, 317. (b) Sarma, B.; Nath, N. K.; Bhogala, B. R.; Nangia, A. *Cryst. Growth Des.* **2009**, *9*, 1546. (c) Childs, S. L.; Stahly, G. P.; Park, A. *Mol. Pharmaceutics* **2007**, *4*, 323.

(6) (a) Flower, R. J. *Pharm. Res.* **1974**, *26*, 33. (b) Moser, P.; Salimann., A.; wissenberg., I. *J. Med. Chem.* **1990**, *33*, 2358. (c) Bowen, E. J.; Eland, J. H. D. *Proc. Chem. Soc.* **1963**, 202. (d) Narsinghania, T.; Chaturvedi, S. C. *Biorg. Med. Chem. Lett.* **2006**, *16*, 461. (e) Peretz, A.; Degani, N.; Nachman, R.; Uziyel, Y.; Gibor, G.; Shabat, D.; Attali, B.

Mol. Pharmacol. **2005**, *67*, 1053. (f) Belsole, S. C.; Chester, N. J. U.S. Patent 1986, 4602040. (g) Philip, J.; Szulczewski, D. H. *J. Pharm. Sci.* **1973**, *62*, 1479. (h) http://www.elephantcare.org/Drugs/meclofen.htm.
(7) (a) http://www.drugbank.ca/drugs/DB00939. (b) http://www.orgyn.com/resources/genrx/D001710.asp.
(8) Fábián, L.; Hamill, N.; Eccles, K. S.; Moynihan, H. A.; Maguire, A. R.; McCausland, L.; Lawrence, S. E. *Cryst. Growth Des.* **2011**, *11*, 3522.
(9) Murthy, H. M. K.; Vijayan, M. *Acta Crystallogr.* **1981**, *B37*, 1102.
(10) Dhanraj, V.; Vijayan, M. *Biochim. Biophys. Acta* **1987**, *924*, 135.
(11) (a) Takasuka, M.; Nakai, H.; Shiro, M. *J. Chem. Soc., Perkin Trans. II* **1982**, 1061. (b) McConnell, J. F.; Company, F. Z. *Cryst. Struct.Commun.* **1976**, *5*, 861. (c) López-Mejías, V.; Kapyf, J. W.; Matzger, A. J. *J. Am. Chem. Soc.* **2009**, *131*, 4554.
(12) (a) Etter, M. C.; Macdonald, J. C. *Acta Crystallogr.* **1990**, *B46*, 256. (b) Bernstein, J.; Davis, R. E.; Shimoni, L.; Chang, N.-L. *Angew. Chem., Int. Ed. Engl.* **1995**, *34*, 1555.
(13) (a) Stahl, P. H., Wermuth, C. G., Eds.; *Handbook of Pharmaceutical Salts: Properties, Selection and Use*; Verlag Helvetica Chimica Acta: Zürich, 2002. (b) Generally Regarded as Safe: http://www.cfsan.fda.gov/~rdb/opa-gras.html and http://www.cfsan.fda.gov/~dms/grasguid. html.
(14) Cambridge Structural Database, Ver. 5.32, 2010, November 2011 update, Cambridge Crystallographic Data Center, UK, www.ccdc.cam.ac.uk.
(15) *Cerius*^{2} *Materials Studio*, http://accelrys.com/products/cerius2, Lattice energy calculation of crystal structures.
(16) Fonari, M. S.; Ganin, E. V.; Vologzhanina, A. V.; Antipin, M. Y.; Kravtsov, V. C. *Cryst. Growth Des.* **2010**, *10*, 3647.
(17) (a) Hathwar, V. R.; Roopan, S. M.; Subashini, R.; Khan, F. N.; Guru Row, T. N. *J. Chem. Sci.* **2010**, *122*, 677. (b) Nath, N. K.; Saha, B. K.; Nangia, A. *New J. Chem.* **2008**, *32*, 1693. (c) Rajput, L.; Chernyshev, V. V.; Biradha, K. *Chem. Commun.* **2010**, *46*, 6530.
(18) (a) Karki, S.; Friščić, T.; Fábián, L.; Jones, W. *CrystEngComm* **2010**, *12*, 4038. (b) Remenar, J. F.; Peterson, M. L.; Stephens, P. W.; Zhang, Z.; Zimenkov, Y.; Hickey, M. B. *Mol. Pharmaceutics* **2007**, *4*, 386. (c) André, V.; Fernandes, A.; Santos, P. P.; Duarte, M. T. *Cryst. Growth Des.* **2011**, *11*, 2325.
(19) (a) Silverstein, R. M. *Spectrometric Identification of Organic Compounds*, 6th ed.; John Wiley & Sons, Inc.: New York, 2002; pp 71−143. (b) Gilpin, R. K.; Zhou, W. *Vib. Spectrosc.* **2005**, *37*, 53. (c) Romero, S.; Escalera, B.; Bustamante, P. *Int. J. Pharm.* **1999**, *178*, 193. (d) Smith, E. Dent, G. *Modern Raman Spectroscopy: A Practical Approach*; John-Wiley: New York, 2005.
(20) (a) Vogt, F. G.; Clawson, J. S.; Strohmeier, M.; Edwards, A. J.; Pham, T. N.; Watson, S. A. *Cryst. Growth Des.* **2009**, *9*, 921. (b) Li, Z. J.; Abramov, Y.; Bordner, J.; Leonard, J.; Medek, A.; Trask, A. V. *J. Am. Chem. Soc.* **2006**, *128*, 8199.
(21) (a) Greco, K.; Mcnamara, D. P.; Bogner, R. *J. Pharm. Sci.* **2011**, *100*, 2755. (b) Murphy, D.; Rodríguez-Cintrón, F.; Langevin, B.; Kelly, R. C.; Rodríguez-Hornedo, N. *Int. J. Pharm.* **2002**, *246*, 121. (c) Ferrari, E. S.; Davey, R. J. *Cryst. Growth Des.* **2004**, *4*, 1061. (d) Cherekuvada, S.; Babu, N. J.; Nangia, A. *J. Pharm. Sci.* **2011**, *100*, 3233. (e) Fini, A.; Cavallari, C.; Bassini, G.; Ospitalli, F.; Morigi, R. *J. Pharm. Sci.* **2012**, DOI: 10.1002/jps.23052.
(22) (a) Friščić, T.; Childs, S. L.; Rizvi, S. A. A.; Jones, W. *CrystEngComm* **2009**, *11*, 418. (b) Alhalaweh, A.; Velega, S. P. *Cryst. Growth Des.* **2010**, *10*, 3302. (c) Rodríguez-Hornedo, N.; Nehm, S. J.; Seefeldt, K. F.; Pagán-Torres, Y.; Falkiewicz, C. J. *Mol. Pharmaceutics* **2006**, *3*, 362. (d) Goud, N. R.; Gangavaram, S.; Suresh, K.; Pal, S.; Manjunatha, N. G.; Nambiar, S. *J. Pharm. Sci.* **2012**, *101*, 664.
(23) Fawzi, M.; Mahjour, M. U.S. Patent, 5,373,022, 1994.
(24) *CrysAlis CCD and CrysAlis RED*, versions 1.171.33.55; Oxford Diffraction: Oxford, 2008.
(25) Diffraction Ltd, Yarnton, Oxfordshire, UK.
(26) Dolomanov, O. V.; Bourhis, L. J.; Gildea, R. J.; Howard, J. A. K.; Puschmann, H. OLEX2: A complete structure solution, refinement and analysis program. *J. Appl. Crystallogr.* **2009**, *42*, 339.
(27) *SMART*, version 5.625 and *SHELX-TL*, version 6.12; Bruker AXS Inc.: Madison, Wisconsin, USA, 2000.
(28) Spek, A. L. *PLATON, A Multipurpose Crystallographic Tool*; Utrecht University: Utrecht, Netherlands, 2002. Single-crystal structure validation with the Program PLATON. *J. Appl. Crystallogr.* **2003**, *36*, 7.
(29) Barbour, L. J. *X-Seed, Graphical interface to SHELX-97 and POV-Ray, Program for Better Quality of Crystallographic Figures*; University of Missouri-Columbia: Missouri, USA, 1999
(30) Kraus, N.; Nolze, G. *Powder Cell, version 2.3, A Program for Structure Visualization, Powder Pattern Calculation and Profile Fitting*; Federal Institute for Materials Research and Testing: Berlin, Germany, 2000.
(31) Glomme, A.; Marz, J.; Dressman, J. B. *J. Pharm. Sci.* **2005**, *94*, 1.